Wetting on cylinders and spheres

Martin P. Gelfand*
Laboratory of Atomic and Solid State Physics, Clark Hall, Cornell University, Ithaca, New York 14853

Reinhard Lipowsky†
Baker Laboratory, Cornell University, Ithaca, New York 14853
(Received 1 May 1987)

A fluid (or Ising-like) system in contact with a uniformly curved substrate, such as a cylinder or sphere, exhibits a surface phase diagram which is different from that when the substrate is flat. Using both an interface model and a Landau theory that includes surface field and surface coupling enhancement parameters, we find that the effects of curvature may be subsumed into an effective bulk (ordering) field. Complete and critical wetting transitions are thus suppressed. At bulk coexistence, the mean-field phase diagram exhibits curvature-induced prewetting and critical prewetting transitions. In $d=3$, finite-size effects smear the prewetting transitions that would otherwise take place in cylindrical or spherical geometries. The Landau theory employs a nonanalytic, piecewise parabolic approximation to the usual quartic polynomial in the free-energy functional. This approximation produces a global surface phase diagram with the correct topology, even though it is unsuited for the description of multicritical phenomena, such as wetting tricriticality. Other strengths and weaknesses of the approximation are described.

I. INTRODUCTION

Interfacial phase transitions[1] and, in particular, wetting transitions of fluids in contact with walls[2] have attracted much attention over the past decade. Most theoretical studies of such transitions have been confined to *planar* substrates. Such a geometry is convenient for calculations, but, from an experimental point of view, cylindrical[3,4] or spherical[5] substrates are also accessible and convenient. In this paper, we give a systematic theoretical description of surface phase transitions for fluid systems with a scalar ($n=1$ component) order parameter on curved substrates. (We do not discuss layering transitions, triple-point wetting, structured fluid-substrate interfaces,[6] and related issues.)

Two basic approaches to the problem are applied here. The first is to retain a fully local description of the system, with configurations specified by the value of an order parameter m at every point $\mathbf{r}$ in space outside the substrate. However, if the system is close to bulk two-phase coexistence, with a layer of the incipient β phase intervening between the substrate, say γ, and the bulk α phase, a simpler description may be contemplated: configurations are described by the height l of the $\alpha\beta$ interface above each point $\boldsymbol{\rho}$ on the substrate surface, while configurations which have overhangs or droplets of one phase in the other are, by the usual arguments,[1] ignored. Such "interface models" have proven useful because they seem to contain all of the physics essential for understanding surface phase transitions. These two theoretical pictures are complementary to a degree. When an interface model can be constructed, it is usually easier to apply than a model for which bulk degrees of freedom must be treated explicitly. However, interface models are unsuited for the description of phenomena where the height of the $\alpha\beta$ interface is ill defined. For example, in the case of near-critical adsorption the only relevant length scale for the order-parameter profile near the substrate is the bulk correlation length. Such phenomena are not considered in this paper.

We first discuss interface models in Sec. II. The effects of substrate curvature can be seen with almost no effort within these models. The next two sections use the other framework, and wetting on curved substrates is studied within the context of simple Landau theory. Section III defines the model, with emphasis on two choices for the bulk Landau free-energy function: the standard analytic m^4 model and a piecewise parabolic "approximation."[7] The familiar planar case is reviewed first in order to compare these two models. Using the latter bulk free-energy function, most quantities of interest can be calculated without recourse to numerics even in curved geometry; see Sec. IV.

Both the interface and Landau-theory approaches lead to the result that the surface phase diagram is severely restricted as a result of the nonplanar geometry; this may be understood by observing that the curved geometry acts like an effective external ordering or bulk field which drives the system away from two-phase coexistence, and thus suppresses critical or complete wetting. Only prewetting transitions, between two β layers of finite thickness, and the associated prewetting critical points remain. For the special case of zero "surface enhancement," this has been seen numerically within the standard Landau theory by Levinson, Jouffroy, and Brochard.[8]

In Sec. V we return to interface models to show that for spherical and cylindrical geometries in dimension $d=3$, finite-size effects suppress the prewetting transitions, at least in principle. In practice one should find

rounded prewetting transitions; the widths of the transitions are calculated explicitly for the case of spheres when the wetting is driven by long-range forces.

We conclude in Sec. VI with a brief summary and some remarks concerning an experiment of Beysens and Estève,[5] who studied a suspension of small silica spheres in a binary-fluid mixture and saw a line of aggregation transitions which they tentatively interpreted as a prewetting line. We suggest that while the aggregation phenomenon is certainly related to the preferential absorption of one component of the mixture at the silica surface, it might not be associated with a prewetting transition as such.

II. INTERFACE MODELS

Hamiltonians for interface models have been constructed in various ways;[7,9–15] these derivations assume that the temperature T is significantly smaller than the bulk critical temperature T_c so that bulk order-parameter fluctuations may be ignored. Interface Hamiltonians generally have the form

$$H_{\rm int}=\int d^{d-1}\rho[\tfrac{1}{2}\Sigma\,|\,\nabla l\,|^2+V(l)]\ , \tag{2.1}$$

where the first term in square brackets is the standard capillary-wave energy, and V is the "interface potential."

The question of what precise form to accept for Σ is not trivial. This issue has been discussed extensively in the context of capillary-wave theory for fluid interfaces.[16–18] In general, Σ is not the surface tension σ that one would measure, say by a capillary-rise experiment, but rather a bare or partially renormalized tension which depends on the short-distance cutoff implicit in the interface Hamiltonian.

The interface potential typically may be expressed as a sum of several kinds of terms which have distinct physical origins. *Short-range* terms, proportional to $e^{-l/\xi}$, $e^{-2l/\xi}$, etc., with ξ the bulk correlation length in the β phase, result from contact interactions between the substrate and fluid. *Long-range* terms, asymptotically proportional to l^{-q}, follow from van der Waals interactions [$q=2,3$ for nonretarded and retarded dispersion forces, respectively, as calculated by Dzyaloshinskii, Lifshitz, and Pitaevskii[19] (DLP)] or unscreened surface ionization forces[20,21] (for which $q=1$). If β is not in bulk coexistence with α, there is a *bulk field* term $l\Delta\Omega$ where $\Delta\Omega$ has units of energy per volume and measures the thermodynamic displacement from bulk $\alpha\beta$ coexistence. Often, close to coexistence, a sensible free energy for the metastable β phase can be estimated, and in such cases $\Delta\Omega$ is just the difference in free-energy densities between β and α.[22] There is always a *hard wall* $V(l<0)=\infty$ so that the interface does not penetrate the substrate.

The mean-field theory of interface models reduces to the study of how the minimum of V and its second derivative there depend on the coefficients of the terms in V. The minimum of V determines the equilibrium wetting-layer thickness $\hat{l}$, while $V''(\hat{l})$ determines the correlation length for interface fluctuations $\xi_\parallel$. Critical behavior in which $\hat{l}$ diverges is described correctly by mean-field theory in $d=3$, provided sufficiently long-range terms are present.[23] Thus $V(l)$, for which in principle the long-range dispersion terms may be calculated by DLP theory,[19] plays a major role in understanding experimental studies of wetting.

So far, we have not included the effects of substrate geometry. However, this is easy to do within an interface model. Suppose that by an appropriate choice of Cartesian coordinates the substrate surface with radius of curvature r_0 can be represented in the form

$$\sum_{i=1}^{\tau+1} x_i^2=r_0^2\ , \tag{2.2}$$

with x_i for $\tau+1<i<d$ unrestricted. Thus in three dimensions $\tau=1$ describes a cylinder while $\tau=2$ specifies a sphere. (Note that $\tau=0$ effectively defines the planar situation.) As the layer thickness l increases for $r_0<\infty$, so does the area of the $\alpha\beta$ interface; since this stretching of the interface is a long-wavelength distortion the resulting term in V should, at first sight, be simply

$$V_\tau(l)=\sigma\left[\left[1+\frac{l}{r_0}\right]^\tau-1\right]\ , \tag{2.3}$$

where, as mentioned, σ is the usual interface tension. This is tantamount to a generalized Laplace's equation. In the context of wetting, this contribution to V has been explicitly taken into account in the experimental work by Taborek and Senator.[4] In fact, this is not completely correct as it stands since there are two physical mechanisms which can make the interface tension radius dependent. The first is asymmetry between the bulk phases, which is present in most real systems and leads to curvature corrections that come as powers of $\delta/(r_0+l)$ where δ is the microscopic Tolman length.[24,25] The second is the finite-size suppression of long-wavelength capillary-wave modes.[18] For our present purposes these corrections to σ may be ignored.

Because V_τ diverges when $l\to\infty$ it is impossible for the equilibrium thickness $\hat{l}$ to become arbitrarily large; this conclusion is clearly not limited to mean-field theory. Thus those transitions in which $\hat{l}$ becomes infinite that occur in planar geometry are lost. This feature will also be seen explicitly in the Sec. IV in the context of Landau theory for the bulk order parameter.

For another comparison with that Landau theory we may estimate the mean-field behavior of $\hat{l}$ at coexistence with only short-range substrate-fluid interactions present. If the leading term in the short-range potential is positive, then for $r_0\gg l\gg\xi$ the dominant terms in V are

$$V(l)\sim C\exp(-l/\xi)+\tau\sigma l/r_0\ ,\quad C>0 \tag{2.4}$$

and in mean-field theory the largest possible wetting-layer thickness is

$$\hat{l}\approx\xi\ln(Cr_0/\tau\sigma\xi)\ . \tag{2.5}$$

This result is only the largest possible thickness because there might be a deeper minimum of V at much smaller l; to say more requires further knowledge of V.

Finally, one might expect some of the terms already present in V for planar geometry to be modified in

curved geometries, specifically those resulting from long-range forces. For dispersion forces, rather than attempt to work out DLP theory in nonplanar geometries, let us apply an approach used by de Gennes.[26] We restrict the considerations to $d=3$. Assume an additive interaction energy between volume elements $d\mathbf{x}$ and $d\mathbf{y}$ located at $\mathbf{x}$ and $\mathbf{y}$ of the form $-c(\mathbf{x})c(\mathbf{y})|\mathbf{x}-\mathbf{y}|^{-p}$. The interaction strength $c(\mathbf{x})$ takes the values c_γ, c_α, and c_β, depending on whether $\mathbf{x}$ lies in the substrate or in the phases α or β. The appropriate value of p is 6 or 7, corresponding to nonretarded or retarded dispersion forces, respectively. In planar geometry, the derivative of the long-range part of V is then

$$V'_{\mathrm{LR}}(l)=-W(p-4)/l^{p-3}\ , \tag{2.6}$$

where W is the standard Hamaker constant[27]

$$W=-2\pi(c_\alpha-c_\beta)(c_\gamma-c_\beta)/(p-2)(p-3)(p-4)\ . \tag{2.7}$$

In spherical geometry, the requisite integrals are all elementary, and the corresponding result is

$$V'_{\mathrm{LR}}(l;r_0)=\frac{-W(p-4)(p-3)(r_0+l)}{r_0^2}\times\left[\frac{r_0+l}{p-3}\left[\frac{1}{l^{p-3}}-\frac{1}{(l+2r_0)^{p-3}}\right]-\frac{1}{p-4}\left[\frac{1}{l^{p-4}}-\frac{1}{(l+2r_0)^{p-4}}\right]\right]\ . \tag{2.8}$$

This is weaker than the result (2.6), as one should expect, since in the curved geometry there is less substrate to participate in the long-range interactions than in a planar geometry. There is no such analytically simple form for $V'_{\mathrm{LR}}(l;r_0)$ for cylindrical substrates, but in both cylindrical and spherical geometries the long-range term decays as $l^{-(p-2)}$ for $l\gg r_0$, that is, one power of l faster than the planar result. Experimental investigation of the regime $l>r_0$ to test the predicted crossover in power laws for V_{LR} would be interesting. It might prove necessary in practice to reduce σ, perhaps by the addition of surfactants, in order to obtain sufficiently thick wetting layers.

III. LANDAU THEORY

A. Introduction

The primary effect of curved substrate geometry that was discussed in the preceding section is the fact that it leads to an additional term in the interface potential caused by the increase in surface area with l. As shown below, this term can also be justified on the basis of a standard Landau theory in which the scalar order parameter, m, is a function of radial distance r. Explicitly, we consider substrates such as spheres or cylinders whose surfaces can be expressed as in (2.2); the distance r is measured from the axis $x_i=0$, for all i with $1\le i\le\tau+1$. Only in these geometries is it possible for the function $m(r)$ alone to give a sensible description of the system.

We will suppose that the fluid-substrate interaction is sufficiently short ranged, so that its effects may be expressed entirely in terms of the surface order parameter $m_1=m(r_0)$, i.e., by a "contact" term. As usual, fluctuations in the order parameter will be neglected, and hence capillary waves are not included in this treatment. Furthermore, the bulk phases in our model will be supposed symmetrically related (as in the simple lattice gas) so there should be no Tolman corrections to the surface tension.[28]

Let f_s denote the surface free energy in units of kT per surface site with area a^{d-1}. The Landau free-energy functional, which is minimized by the equilibrium order-parameter profile, can be put in the general form

$$f_s\{m(r)\}=f_1(m_1)+\int_{r_0}^{\infty}\left[\frac{1}{a}f[m(r)]+\frac{a}{2}\left[\frac{dm}{dr}\right]^2\right]\left[\frac{r}{r_0}\right]^{\tau}dr\ . \tag{3.1}$$

Although $f_s\{m(r)\}$ represents the surface free energy only after it has been minimized, we will often use the term "free energy" to denote this functional evaluated for an explicitly specified order-parameter profile. The factors $1/a$ and $a/2$ are convenient but otherwise arbitrary—they are fixed so that in conjunction with a similar choice for the coefficient of m^4 in (3.4), the bulk-correlation-length amplitude is a in the disordered phase and the order-parameter amplitude is unity. Note that m, f, and f_1 are all dimensionless. For the contact energy $f_1(m_1)$, which represents the fluid-substrate interaction, we take[29]

$$f_1(m_1)=-h_1m_1-\tfrac{1}{2}gm_1^2\ . \tag{3.2}$$

In magnetic terms, h_1 may be thought of as a field applied only to the surface spins, while g is a measure of the enhanced (or de-enhanced) coupling between surface spins.

If f_s is to represent the surface free energy, the bulk free-energy function $f(m)$ in (3.1) must satisfy

$$f(m(\infty))=0\quad\text{where } m(\infty)\text{ minimizes } f(m)\ . \tag{3.3}$$

The standard phenomenological choice for the form of $f(m)$, which we will refer to as the "smooth f," is

$$f(m)=-\tfrac{1}{2}tm^2+\tfrac{1}{4}m^4+hm-f_0\ , \tag{3.4}$$

with $f_0(t,h)$ chosen to satisfy (3.3). Note that, contrary to usual practice, the reduced temperature, t, is taken positive for two-phase coexistence, while the sign of the hm term is opposite that of the h_1m_1 term in f_1: these conventions are convenient since in the interesting part of the phase diagram h, t, and h_1 are then all positive.

Inspection of the equations above reveals that the surface free energy may be written in a scaled form. For $t>0$ we define a set of scaled order-parameter, field, and free-energy variables

$$M=m/t^{1/2},\quad M_1=m_1/t^{1/2},$$
$$H=h/t^{3/2},\quad G=g/t^{1/2},\quad H_1=h_1/t, \tag{3.5}$$
$$F_s=f_s/t^{3/2},\quad F_1=f_1/t^{3/2},\quad F=f/t^2$$

and scaled radial distance and substrate radius variables

$$R=\sqrt{2}t^{1/2}r/a,\quad R_0=\sqrt{2}t^{1/2}r_0/a\ . \tag{3.6}$$

Then the functional (3.1) may be rewritten as

$$F_s\{M(R)\}=F_1(M_1)+\frac{1}{\sqrt{2}}\int_{R_0}^{\infty}\left[F(M)+\left[\frac{dM}{dR}\right]^2\right]\left[\frac{R}{R_0}\right]^{\tau}dR\ , \tag{3.7}$$

with

$$F_1(M_1)=-H_1M_1-\tfrac{1}{2}GM_1^2\ , \tag{3.8}$$

and

$$F(M)=-\tfrac{1}{2}M^2+\tfrac{1}{4}M^4+HM+F_0\ . \tag{3.9}$$

Thus the surface phase diagram of Nakanishi and Fisher[29] for this model (in planar geometry) in the half-space $(t>0,h,h_1,g)$ may be displayed in one diagram in the space (H,H_1,G); such a phase diagram is sketched in Fig. 1. Even using the scaled variables, the full phase diagram in curved geometries is four dimensional since another axis enters for the scaled substrate radius R_0.

In general, the functional F_s is made extremal, though not necessarily minimal, by solutions of the Euler equation

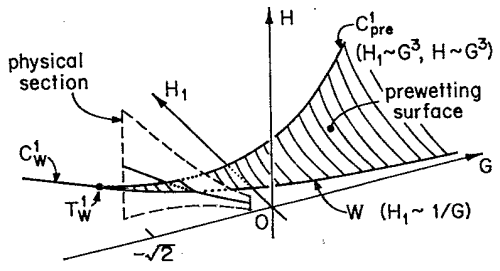

FIG. 1. Sketch of the scaled surface phase diagram using the smooth free-energy function F, (3.9), for $H_1\geq 0$ in the two-phase region of the bulk phase diagram $(t>0)$ (following Ref. 29). The diagram for $H_1\leq 0$ is obtained by rotating the displayed region about the G axis by 180°. As in Ref. 29, the symbols C^1_W, T^1_W, W, and C^1_{pre} denote critical wetting, tricritical wetting, first-order wetting, and critical prewetting, respectively. Also shown is a typical "physical section" of the phase diagram in which h_1 and g are held fixed while t and h are varied. Not indicated explicitly, except in the physical section, are the first-order transitions which comprise the part of the $H=0$ plane between the wetting line and the G axis and the continuous transitions (complete wetting) which comprise the remainder of the $H=0$ plane.

$$\frac{d^2M}{dR^2}+\frac{\tau}{R}\frac{dM}{dR}=\frac{1}{2}\frac{dF}{dM}\ , \tag{3.10}$$

subject to boundary conditions at infinity, namely,

$$F(M(\infty))=0\ , \tag{3.11}$$

the scaled version of (3.3), and at the substrate surface, namely,

$$\sqrt{2}\frac{dM}{dR}\bigg|_{R=R_0}=\frac{dF_1}{dM_1}\ . \tag{3.12}$$

However, the functional minimization can be accomplished in other ways. The method we will apply is to find a family of profiles $M(R)$ which satisfy (3.10) and (3.11)—but not necessarily (3.12). The members of such a family may typically be specified by a single parameter. The free-energy functional (3.7), including the boundary term, is evaluated for the members of this family and minimized by the usual methods for minimizing a *function,* since $F_s\{M(R)\}$ now depends, in effect, on only one variable. There are several advantages of this approach over the usual one. (a) Minima are more readily distinguished from maxima and saddle points. (b) It is easy to see when the free-energy functional becomes unbounded below [so that no solution of the Euler equation subject to the usual boundary conditions (3.11) and (3.12) is the global minimum]. This unphysical situation will arise in part of the surface phase diagram as a consequence of the approximation described in the next paragraph. (c) The boundary condition at the substrate surface serves as an independent check, since it will generally be satisfied by the equilibrium profile. Finally, if there are several competing minima, one will need to evaluate the free-energy functional for various $M(R)$ even within the usual approach. Thus our method requires no more calculation than the usual one, at least when the calculations are done analytically rather than numerically.

B. Double-parabola approximation

Unfortunately, for $\tau>0$ the differential equation (3.10) with the smooth F, (3.9), defies exact solution. If dF/dM were linear in M, the equation could be easily solved in terms of modified Bessel functions. Thus one is motivated[30] to approximate the smooth F in a piecewise parabolic fashion. For $H=0$, the simplest choice is

$$F=(M\mp 1)^2,\quad M\gtrless 0\ , \tag{3.13}$$

which has minima and second derivatives at the minima which match those of (3.9). For $H\neq 0$, there are several conceivable extensions of this approximation. The most straightforward is to add HM to (3.13) and adjust the "constant" F_0 to satisfy (3.3). A further shift in M yields the $F(M)$ which we will adopt as the "double-parabola approximation," or DPA,[7] namely,

$$F=\begin{cases}(M+1)^2, & M<H/2\\ (M-1)^2+2H, & M>H/2\end{cases} \tag{3.14}$$

where it has been assumed that $H>0$. In this model, the thermodynamic displacement from coexistence, $\Delta\Omega$

of Sec. II, is directly proportional to the scaled bulk field H and is given explicitly by $\Delta\Omega = 2Ht^2(kT/a^d)$.

C. Planar case

It is informative in the first place to compare the phase diagrams for the Landau theory in the standard planar geometry using both the smooth F and the DPA. The solutions of (3.10) with the DPA are not controlled approximations to solutions with the smooth F. However, we may expect the approximation to get some features of the phase diagram qualitatively correct: it should do particularly well near coexistence, where the order-parameter profiles are dominated by the shape of F near its minima. Thus the behavior of the prewetting surface at small H should be described correctly by the DPA. The DPA serves as a poor approximation to the smooth F when the details of the behavior near its cusp are important as, for example, at critical prewetting.

When $\tau = 0$, the differential equation (3.10) has a first integral[2] and calculation of the surface phase diagram for any F reduces to a problem in finding roots, differentiation, and quadrature. Surface phase diagrams calculated in that way for the smooth F and the DPA are sketched in Figs. 1 and 2, respectively. The critical wetting lines are the same in both cases,[7] but the critical wetting, first-order wetting, and critical prewetting lines in the DPA meet with unphysical discontinuities in slope at the wetting tricritical point. The approximation is thus not useful for studying tricritical or higher-order multicritical phenomena. The behavior at the other endpoint of the DPA wetting curve is also unphysical, as will be discussed in more detail below.

Another way to calculate the surface phase diagram for the DPA was described after Eq. (3.12). This method is briefly sketched here since it is readily generalized to $\tau \neq 0$. The general solution to (3.10) is

$$M(R) = \begin{cases} A_+ e^R + A_- e^{-R} + 1, & M \geq H/2 \\ B_+ e^R + B_- e^{-R} - 1, & M \leq H/2 \end{cases} \tag{3.15}$$

where $A_\pm$ and $B_\pm$ are constants of integration. However, the continuity of $M(R)$ and $M'(R)$ when $M = H/2$ must be required, and the boundary condition (3.11) must be satisfied. When $H = 0$ the DPA has two equivalent minima, at $M = \pm 1$; in that case assume $H = 0^+$ so that $M(\infty) = -1$. If, as explained, we now neglect the boundary condition at the substrate surface, for $H > 0$ there are two classes of solutions in $0 \leq R < \infty$: (i) "dry," with $M \leq H/2$ everywhere, and (ii) "wet," with the scaled surface order parameter $M_1 > H/2$ so there exists a "connection point" $R_c > 0$ where $M(R_c) = H/2$. At coexistence, a free interface at infinity between the $M = \pm 1$ phases contributes only a finite amount $(\sqrt{2})$ to the scaled free energy F_s; thus when $H = 0$ one must also consider a third class of solutions: "completely wet," with $M_1 \geq 1$, and $M(\infty) = 1$. Each class of solutions is a one-parameter family of functions whose free energies are easily evaluated. Thus, as anticipated, a functional minimization problem has been turned into a problem of minimizing a few functions of a single variable.[31]

In the remainder of this section, we consider aspects of the DPA in planar geometry for comparison with related results in curved geometries that will be derived in Sec. IV.

1. *The unphysical region and F_{dry}*

Consider the dry solutions:

$$M(R) = B_- e^{-R} - 1, \quad B_- \leq 1 + H/2 \tag{3.16}$$

where the constraint on B_- ensures that $M_1 \leq H/2$. When the free energy is evaluated as a function of B_-, one obtains

$$F_{\rm dry}(B_-) = \tfrac{1}{2}(\sqrt{2} - G)B_-^2 + (G - H_1)B_- + (H_1 - \tfrac{1}{2}G) . \tag{3.17}$$

Thus (a) when $G < \sqrt{2}$ the minimum dry solution is given by

$$B_- = B_-^* \equiv (H_1 - G)/(\sqrt{2} - G) , \tag{3.18}$$

in agreement with the solution of the boundary condition (3.12) using the form (3.16) for $M(R)$, provided that $B_-^* \leq 1 + H/2$. If this latter condition is violated, the smallest $F_{\rm dry}$ is achieved with $B_- = 1 + H/2$.[32] However, (b) for $G > \sqrt{2}$ the coefficient of B_-^2 in (3.17) is negative so the free energy is unbounded below as B_- diverges to $-\infty$: this corresponds to the unphysical region indicated in Fig. 2. The smooth F avoids this catastrophe because the M^4 term causes the integral contribution to the free energy, which is

$$B_-^2/\sqrt{2} = (M_1 + 1)^2/\sqrt{2}$$

in (3.17), to grow faster than quadratically as $M_1 \to -\infty$.

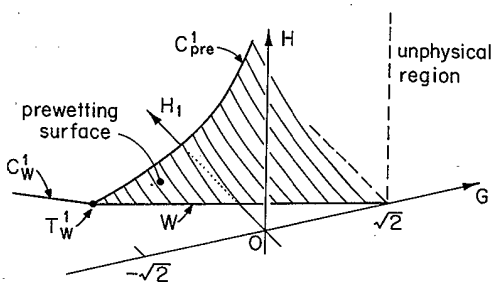

FIG. 2. Sketch of the scaled surface phase diagram based on the double-parabola approximation, (3.14), using the same conventions and notation as in Fig. 1. In the half-space $G \geq \sqrt{2}$, the approximation gives unphysical results. In addition, as $G \to \sqrt{2}$ along the prewetting critical line [Eq. (3.24)] H diverges to $+\infty$ while H_1 remains finite. Note that at bulk coexistence ($H = 0^\pm$) in curved geometries, one finds qualitatively the same phase diagram if the $(\pm)H$ axis is relabeled τ/R_0; indeed, the agreement is quantitative sufficiently close to the (H_1, G) plane.

2. *Wet solutions and prewetting at small H*

Wet solutions are given by (3.15) with the coefficients determined by the continuity of M and its first derivative when $M=H/2$, that is, at $R=R_c$. This "connection point" is also a good measure of the scaled wetting-layer thickness L, so in the planar case we set $L=R_c$. A simple calculation leads to an expression for the surface free energy for wet solutions parametrized by L, which we write as[33]

$$F_{\rm wet}(L)=F_1(M_1)+\frac{1}{\sqrt{2}}[2+H+2HL +(M_1+e^{-L}-1)^2-e^{-2L}] \tag{3.19}$$

where

$$M_1=M(R=0)=1-e^{-L}+\tfrac{1}{2}He^{L}\ . \tag{3.20}$$

For $H_1>-G>\sqrt{2}$ and small H, the value of L which minimizes the free energy is found to be

$$L_w\simeq L_w^0=\ln(A/H),\quad A=2(H_1+G)/(\sqrt{2}-G) \tag{3.21}$$

as expected on the basis of a phenomenological interface potential [recall Eq. (2.5)].

The prewetting surface is characterized by equilibrium between wet and dry order-parameter profiles, i.e., $F_{\rm wet}(H_1,G,H)=F_{\rm dry}(H_1,G,H)$. This surface is bounded on one side by the wetting curve and on the other by the locus of prewetting critical points. To calculate the prewetting surface at small H, near the wetting curve, it is enough to retain the dominant terms in $F_{\rm wet}$ for $L\simeq L_w^0$, namely,

$$F_{\rm wet}(L)\approx-\tfrac{1}{2}H(H_1+G)e^{L}+\tfrac{1}{8}H^2(\sqrt{2}-G)e^{2L}+\sqrt{2}HL\ . \tag{3.22}$$

The first two terms alone determine L_w^0, while the last is required in order that the approximate free energy reproduce the leading variation with H. Then one may set $F_{\rm dry}(B_{\pm}^{*})=F_{\rm wet}(L_w^0)$ and use the fact that the prewetting surface at small H is close to the wetting curve so that $H_1\approx(\sqrt{2}-G)/2$. The result is the prewetting surface

$$H_1=\tfrac{1}{2}(\sqrt{2}-G)\left[1+H\left[\ln\frac{(\sqrt{2}+G)/(\sqrt{2}-G)}{H} +O(H^0)\right]\right]\ . \tag{3.23}$$

The $H\ln H$ dependence of the prewetting surface as $H\to0$ reflects the thermodynamic requirement,[34] a "Clapeyron" relation, associated with (3.21).

3. *The prewetting critical line*

As the locus of prewetting critical points is approached along the prewetting surface, the wet and dry order-parameter profiles in equilibrium with each other merge into a single profile. The equation of this locus for the DPA is

$$H_1=G+2\sqrt{2},\quad H=2(\sqrt{2}+G)/(\sqrt{2}-G),\quad -\sqrt{2}<G<\sqrt{2}\ . \tag{3.24}$$

This result may be derived from either the first-integral method mentioned above[2] or the simultaneous solution of two relations which must hold on the prewetting critical locus, namely, $F'_{\rm wet}(L=0)=0$ and $F''_{\rm wet}(L=0)=0$. (These assert that the minimal wet profile satisfies $M_1=H/2$; furthermore, the former is equivalent to the condition $B_{\pm}^{*}=1+\frac{1}{2}H$ and thus the minimal dry profile also has $M_1=H/2$.) A comparison of (3.23) with (3.24) reveals that the value of H as a function of G along the prewetting critical locus is a relevant scale for H.

IV. DOUBLE-PARABOLA APPROXIMATION IN CURVED GEOMETRIES

The program which was carried out in Sec. III C for planar geometry will now be implemented in curved geometries. For simplicity, the calculations will be performed at bulk coexistence, with $H=0^{+}$. The main goals of this exercise are to show (i) that for large enough R_0 the effects of curvature are identical to those produced by a bulk field, with the effective H given by $H_{\rm eff}=\tau/R_0$ in accord with the interface model of Sec. II, and (ii) that the topologies of the phase diagrams in the spaces $(H_1,G,H,1/R_0=0)$ and $(H_1,G,H=0,1/R_0)$ are the same. These features of wetting on curved substrates should hold for any sensible choice of F. We will also examine the interesting, unexpected, but probably model-dependent behavior of the curvature-induced prewetting critical locus as a function of τ.

A. General solutions for arbitrary $\tau>0$

The first step is the calculation of explicit forms for order-parameter profiles, which are solutions of

$$\frac{d^2M}{dR^2}+\frac{\tau}{R}\frac{dM}{dR}=M\mp1,\quad M\gtrless0 \tag{4.1}$$

with $M(\infty)=-1$. Unlike the planar case, there are only two classes of solutions at coexistence, namely, "dry" ones, with $M\le0$ everywhere, and "wet" ones, which cross $M=0$ at $R_c\ge R_0$. The third class of solutions that arose in the planar case, those with an interface at infinity, are lost in the curved geometries since the free energy per surface site diverges as the interface is pushed to infinity.

The general solution of (4.1) for unrestricted M is the sum of the particular solutions $M=\pm1$ and the general solution of the homogeneous equation

$$\frac{d^2M}{dR^2}+\frac{\tau}{R}\frac{dM}{dR}=\left[1+\frac{\nu(\nu+\tau-1)}{R^2}\right]M\ , \tag{4.2}$$

with the order ν set to zero. It is easily verified that two independent solutions of this equation are

$$\mathcal{J}_\nu(R)=I_{(\nu+p)}(R)/R^p,\quad \mathcal{H}_\nu(R)=K_{(\nu+p)}(R)/R^p\ , \tag{4.3}$$

with $p=\frac{1}{2}(\tau-1)$ while I and K are the standard modified Bessel functions.[35] Note that the geometric pa-

rameter τ has been suppressed; when no argument is indicated it should be assumed to be R. A subscript 0 will denote evaluation at $R=R_0$, for example, $\mathcal{K}_{10}=\mathcal{K}_1(R_0)$; likewise, a subscript c will denote evaluation at $R=R_c$. These functions satisfy recursion, derivative, and Wronskian relations analogous to those for the usual modified Bessel functions, which are useful in several of the calculations described below.

The general solution to (4.1) may now be written as

$$M(R)=\begin{cases}1+\mathcal{A}_-\mathcal{K}_0+\mathcal{A}_+\mathcal{I}_0, & M\geq 0\\ -1+\mathcal{B}_-\mathcal{K}_0, & M\leq 0\end{cases} \tag{4.4}$$

where $\mathcal{A}_\pm$ and $\mathcal{B}_-$ are constants of integration. Consider first dry solutions.

B. Dry solutions

Order-parameter profiles that never cross $M=0$ are given by

$$M(R)=\mathcal{B}_-\mathcal{K}_0-1, \quad \mathcal{B}_-\leq 1/\mathcal{K}_{00} . \tag{4.5}$$

Inserting this into (3.7) and carrying out the integration yields

$$F_{\rm dry}(\mathcal{B}_-)=F_1(\mathcal{B}_-\mathcal{K}_{00}-1)+\frac{1}{\sqrt{2}}\mathcal{B}_-^2\mathcal{K}_{00}\mathcal{K}_{10} . \tag{4.6}$$

The minimal dry solution is given by

$$\begin{aligned}\mathcal{B}_- &= \min(\mathcal{B}_-^*, 1/\mathcal{K}_{00}) ,\\ \mathcal{B}_-^* &= (H_1-G)/(\sqrt{2}\mathcal{K}_{10}-G\mathcal{K}_{00}) ,\end{aligned} \tag{4.7}$$

provided $G<\sqrt{2}\mathcal{K}_{10}/\mathcal{K}_{00}\equiv S$. For $G>S$ the DPA breaks down in the previous way; thus there is an unphysical wedge in the space $(H_1, G, 1/R_0)$.

To calculate the curvature-induced prewetting surface at large R_0, the asymptotic expansions of the modified Bessel functions at large argument can be used to obtain an approximate expression for $F_{\rm dry}(\mathcal{B}_-^*)$. It is sufficient for our purposes to note that $\mathcal{K}_{10}/\mathcal{K}_{00}=1+\tau/2R_0+O(R_0^{-2})$. Then, if $\bar{F}_{\rm dry}$ denotes the free energy in a planar geometry [see (3.7)], we obtain

$$F_{\rm dry}(\mathcal{B}_-^*)=\bar{F}_{\rm dry}(B_-^*)+O(R_0^{-1}) \tag{4.8}$$

where B_-^* is given in (3.18).

C. Wet solutions

Wet solutions cross the M axis at R_c, and this connection point provides the natural parametrization of the solutions. The matching conditions at R_c, namely, $M(R_c^+)=M(R_c^-)=0$ and $M'(R_c^+)=M'(R_c^-)$, lead to the relations

$$\begin{aligned}&\mathcal{A}_+=-2R_c^\tau\mathcal{K}_{1c}, \quad \mathcal{A}_-=R_c^\tau(\mathcal{I}_0\mathcal{K}_1-\mathcal{I}_1\mathcal{K}_0)_c/\mathcal{K}_{0c} ,\\ &\mathcal{B}_-=1/\mathcal{K}_{0c} ,\end{aligned} \tag{4.9}$$

between R_c and the constants in (4.4).

With $\mathcal{A}_\pm$ and $\mathcal{B}_-$ specified as here, one can write down $F_{\rm wet}$ using (3.7). That integral can be evaluated exactly with the result

$$\begin{aligned}F_{\rm wet}(R_c)=&-F_1(M_1)+\frac{1}{\sqrt{2}}R_0^{-\tau}\{R_c^\tau\mathcal{K}_{1c}/\mathcal{K}_{0c}+\mathcal{A}_+^2[(R^\tau\mathcal{I}_0\mathcal{I}_1)_c-(R^\tau\mathcal{I}_0\mathcal{I}_1)_0]+\mathcal{A}_-^2[(R^\tau\mathcal{K}_0\mathcal{K}_1)_0-(R^\tau\mathcal{K}_0\mathcal{K}_1)_c)]\\ &+\mathcal{A}_+\mathcal{A}_-[R_0^\tau(\mathcal{I}_0\mathcal{K}_1-\mathcal{I}_1\mathcal{K}_0)_0-R_c^\tau(\mathcal{I}_0\mathcal{K}_1-\mathcal{I}_1\mathcal{K}_0)_c]\} ,\\ M_1=&\mathcal{A}_+\mathcal{I}_{00}+\mathcal{A}_-\mathcal{K}_{00}+1 .\end{aligned} \tag{4.10}$$

This is not at all illuminating. But, in the limit of large R_0, asymptotic expansions for the modified Bessel functions are again applicable, and $F_{\rm wet}$ may be expressed more simply. If one defines the scaled wetting-layer thickness by

$$L=R_c-R_0 , \tag{4.11}$$

and assumes $L\ll R_0$, the asymptotic expansion may be followed by a Taylor expansion in L/R_0. Then the dominant terms in the expansion of the free energy are

$$\begin{aligned}F_{\rm wet}(L)\approx&-\frac{1}{2}\frac{\tau}{R_0}(H_1+G)e^L\\ &+\frac{1}{8}\left[\frac{\tau}{R_0}\right]^2(\sqrt{2}-G)e^{2L}+\sqrt{2}\frac{\tau}{R_0}L .\end{aligned} \tag{4.12}$$

Comparing this with (3.22), one sees that when R_0 is large, τ/R_0 *plays the same role as a bulk field* H. Furthermore, since $F_{\rm dry}(\mathcal{B}_-^*)-\bar{F}_{\rm dry}(B_-^*)=O(R_0^{-1})$ [recall (4.8)] rather than $O(\ln R_0^{-1})$, the curvature-induced prewetting surface for small $1/R_0$ is given by (3.23), with H there replaced by the effective bulk field τ/R_0.

In fact, τ/R_0 is *exactly* what one expects as the effective bulk field, on the basis of the simple interface model. Let us modify the definition of the interface potential V given in Sec. II somewhat, and take it to have units of kT per surface site, as does f_s. The standard bulk field term becomes $2ht^{1/2}l/a$, while the leading curvature-induced term for $l\ll r_0$ is $\tau\sqrt{2}t^{3/2}l/r_0$, since the tension of a free planar interface is $\sqrt{2}t^{3/2}$. Equating these two terms and using the definitions (3.5) and (3.6) of the scaled variables leads to the identification of τ/R_0 as the effective H.

D. Curvature-induced prewetting and prewetting criticality

Now we would like to see that the topology of the phase diagram in the space $(H_1, G, 1/R_0)$ is the same as that of phase diagram in the space $(H_1, G, H \geq 0)$. For sufficiently small $1/R_0$ we have seen that the two phase diagrams are identical. Farther away from $1/R_0 = 0$, the problem of calculating the equilibrium wetting-layer thicknesses and the loci of phase equilibria is more difficult.

Outside the unphysical wedge $G > \sqrt{2}\mathcal{H}_{10}/\mathcal{H}_{00}$, and for $1/R_0 > 0$, the free energy $F_{\rm wet}(R_c)$ diverges to $+\infty$ as $R_c \to \infty$. Therefore any surface phase transitions in curved geometries are prewetting transitions between phases of different finite wetting-layer thicknesses. Numerical minimization of (4.10) and comparison with the minimized $F_{\rm dry}(\mathcal{B}_-)$ confirms for $\tau = 1$ and 2, and there is no reason to doubt for general τ, that there is a curvature-induced prewetting surface, satisfying $F_{\rm wet} = F_{\rm dry}$, extending from the wetting curve on the $1/R_0 = 0$ plane. The prewetting critical locus which terminates the surface is found by evaluating the wetting-layer thickness L_w for the wet profiles on this surface and extrapolating it to zero, say as a function of H_1 and R_0 at fixed G. A sketch of the resulting phase diagram is unnecessary since it is essentially the same as Fig. 2 if the label on the positive H axis there is changed to $1/R_0$. Of course, the phase diagrams have different unphysical regions and consequently their prewetting surfaces behave differently at "large" G (say, $G > 1$) where the unphysical divergences in $F_{\rm wet}$ and $F_{\rm dry}$ begin to determine the behavior; however, these distinctions are not of physical interest.

It is conceivable that in curved geometries there could be additional first-order transitions between pairs of wet profiles, so that the proposed phase diagram would be incomplete. We have not ruled out this possibility entirely, but it does not seem at all plausible. Numerical evaluation of (4.10) for $\tau = 1, 2$ at a variety of points in the space $(H_1, G, 1/R_0)$ suggests that $F_{\rm wet}(R_c)$ has at most one minimum for $R_c > R_0$, and thus equilibria between distinct wet solutions is not possible.

The numerical calculations of the prewetting critical locus for $\tau = 1, 2$ reveal a surprising feature: their projections onto the (H_1, G) plane seem to be identical. We know of no reason to expect this; however, a proof that these projections are indeed independent of τ is straightforward. As in the planar case, two independent conditions which together specify prewetting criticality are $F'_{\rm wet}(L = 0) = 0$, which implies

$$-H_1 + \sqrt{2}T = 0 \quad \text{where } T = \mathcal{H}_{10}/\mathcal{H}_{00} , \tag{4.13}$$

and $F''_{\rm wet}(L = 0) = 0$, which implies

$$-H_1\left[-3 - \frac{\tau}{R_0}T + 2T^2\right] - GT^2 + \frac{1}{\sqrt{2}}\left[-10T - \frac{2\tau}{R_0}T^2 + 6T^3\right] = 0 . \tag{4.14}$$

When these equations are combined to eliminate T, the resulting projection of the critical prewetting locus onto the (H_1, G) plane, namely,

$$H_1 = G/2 + [(G/2)^2 + 4]^{1/2} \quad \text{with } G > -\sqrt{2} , \tag{4.15}$$

lacks any τ dependence.

V. FINITE-SIZE EFFECTS

We have seen that on curved substrates the only surface phase transitions are prewetting and critical prewetting transitions, since surface tension prevents wetting-layer thicknesses from diverging. In this section we point out that in $d = 3$ and for $\tau = 1, 2$—that is, for cylinders and spheres—even these transitions do not strictly exist because of finite-size effects.

As Nakanishi and Fisher[29] emphasize, prewetting criticality contains as a special case supercritical surface enhancement (in a ferromagnet, this corresponds to the surface having a higher Curie temperature than the bulk) and hence the universality class for both is the $(d-1)$- (here, two-) dimensional Ising class. Within the context of interface models the universality-class assignment is clear. The order parameter l is a scalar, and a prewetting transition corresponds to a double-well structure in the interface potential $V(l)$. As prewetting criticality is approached along the prewetting surface, the wells move closer together and the barrier between them shrinks.

For curved geometries in $d = 3$, a prewetting transition would be tantamount to an Ising transition in a finite system (a sphere) or in an infinite strip (cylinder). Neither of these transitions can occur for $T > 0$; thus the prewetting surface and its associated critical points cannot exist as sharp transitions. What one should see instead are rounded transitions. For any $d > 3$, the same mechanism rounds the prewetting transitions when $\tau = d - 1$ or $d - 2$.

The theory of finite-size scaling at first-order transitions, which provides a scheme for calculating the widths of these rounded phase transitions when r_0 is sufficiently large, is succinctly reviewed by Privman and Fisher.[36] One needs at least three basic ingredients: the temperature, T, the substrate radius, r_0, and the free-energy difference per unit area between the thick and thin layers (i.e., the surface phases that coexist at prewetting), $\Delta\Omega_s$, as a function of whatever thermodynamic fields are being adjusted so as to cause prewetting. The surface free-energy difference here is analogous to the bulk free-energy difference $\Delta\Omega$ mentioned in Sec. II, since in both cases one of the phases will be metastable. However, reasonably direct control can be exerted on $\Delta\Omega$, at least when it is small. For a magnetic system, $\Delta\Omega$ is initially linear in the applied field. For a binary-fluid mixture at fixed composition and close to bulk two-phase equilibrium, $\Delta\Omega$ is proportional to $T - T^*$, where T^* is the temperature at which coexistence is attained. In both cases, the constants of proportionality can at least in principle be determined by bulk thermodynamic measurements. In contrast, $\Delta\Omega_s$ is not directly accessible; even crude estimates are impossi-

ble without some knowledge of the interface potential $V(l)$.

Rounding of first-order transitions on the surface of a sphere has not been studied explicitly, but one expects that the surface of a sphere in d dimensions of radius r_0 has roughly the same finite-size behavior as an r_0^{d-1} block subject to periodic boundary conditions. With this assumption, the rounded prewetting region for $\tau=d-1$ is determined by

$$|\Delta\Omega_s| r_0^{d-1} \lesssim kT . \tag{5.1}$$

The cylindrical $r_0^{d-2}\times\infty$ geometry has been studied explicitly.[36] To calculate the width of the transition in this case, the domain-wall free energy, say Σ_s, between regions with different wetting-layer thicknesses, and the bulk correlation length ξ, which serves as the elementary length scale for interface models, are required in addition to T, r_0, and $\Delta\Omega_s$. The rounded prewetting region is then[36]

$$|\Delta\Omega_s| r_0^{d-2}\xi \exp(r_0^{d-2}\Sigma_s/kT) \lesssim kT . \tag{5.2}$$

For the important case of wetting on spheres in $d=3$ driven by long-range forces, close to the wetting transition (and therefore near bulk coexistence specified by $\Delta\Omega=0$) the mean-field behavior of the interface models allows one to estimate $\Delta\Omega_s$ and thence the width of the rounded prewetting transition. Suppose that one has under control $\Delta\Omega$ and another parameter such as the temperature T. For $\xi \ll l \ll r_0$ the interface potential takes the form

$$V(l) \simeq W/l^q + (\Delta\Omega + 2\sigma/r_0)l . \tag{5.3}$$

The Hamaker constant W may be estimated from experiments in planar geometry,[37,38] and in general it depends only weakly on T in the vicinity of the wetting transition.[39] Suppose $\Delta\Omega_{\rm pre}$ is the value of $\Delta\Omega$ as a function of T along the mean-field prewetting line, on which V has two equal local minima and $\Delta\Omega_s=0$. One of these minima corresponds to a thin wetting layer of width l_d, while the other corresponds to a thick one of width l_w, where (5.3) is valid with $W>0$. The change in $V(l)$ as $\Delta\Omega$ moves away from $\Delta\Omega_{\rm pre}$ is much greater for large l than for small l, so to leading order in the bulk thermodynamic distance from prewetting, $\Delta\Omega-\Delta\Omega_{\rm pre}$, the surface free-energy difference is

$$\begin{aligned}\Delta\Omega_s &\simeq V(l_w;\Delta\Omega) - V(l_w;\Delta\Omega_{\rm pre}) \\ &\simeq (\Delta\Omega-\Delta\Omega_{\rm pre})[(\Delta\Omega_{\rm pre}+2\sigma/r_0)/qW]^{-1/(q+1)} .\end{aligned} \tag{5.4}$$

Then the rounded width of the prewetting transition along the $\Delta\Omega$ direction is given by

$$\delta_{\rm fs}(\Delta\Omega) \simeq kTr_0^{-2}[(\Delta\Omega_{\rm pre}+2\sigma/r_0)/qW]^{1/(q+1)} . \tag{5.5}$$

As expected, this shrinks to zero as the radius r_0 increases. This expression becomes simpler when the surface stretching term $2\sigma/r_0$ may be ignored, such as in finite planar geometries, or when $\Delta\Omega_{\rm pre} \gg 2\sigma/r_0$. In addition, under such conditions the prewetting line has a power-law behavior:[34]

$$\Delta\Omega_{\rm pre} \sim |T-T_W|^{(q+1)/q} \tag{5.6}$$

where T_W refers to the temperature at the wetting transition. Thus for any value of q, the fractional rounding $\delta_{\rm fs}(\Delta\Omega)/\Delta\Omega_{\rm pre}$ becomes proportional to $|T-T_W|^{-1}$.

It seems unlikely that finite-size rounding could ever interfere with experimental attempts to demonstrate the existence of a prewetting transition. For illustrative purposes, we again consider only spherical geometry and interface potentials described by (5.3) at large distances. The width of the transition $\delta_{\rm fs}(\Delta\Omega)$ due to finite-size rounding must be compared with the best experimental resolution $\delta_{\rm ex}(\Delta\Omega)$ available. Both of these quantities will depend strongly on the details of the system being studied; here we imagine a representative binary-fluid mixture not too close to its consolute point. It is characterized by $kT\simeq 3\times10^{-14}$ erg (around room temperature), $q=2$ and $W\simeq 10^{-16}$ erg (drawn loosely from Ref. 38), and $\sigma\simeq 1$ erg/cm^2. It is difficult to offer even an order-of-magnitude estimate for $\Delta\Omega_{\rm pre}$; for the moment it is neglected. The rounding $\delta_{\rm fs}$ is then bounded below by roughly $5\times10^{-9}(r_0/1\text{ cm})^{-2.3}$ erg/cm^3.

In binary-fluid mixtures, $\Delta\Omega$ has been successfully manipulated by two different methods. In the first,[38] the mixture is actually at bulk coexistence, but the substrate is at some vertical distance z from the bulk meniscus. Then $\Delta\Omega=g\Delta\bar{\rho}z$, where g is the gravitational acceleration and $\Delta\bar{\rho}$ is the mass density difference between the two bulk phases (which we set to 0.1 gm/cm^3 for our present purposes). One could imagine studying wetting layers on a suspension of spheres in a mixture at coexistence by turbidity measurements[5] with a vertical resolution of about 1 mm, though "practical" matters such as aggregation[5] and long equilibriation times[40,41] could make such an experiment impossible to carry out. Hypothetically, at least, $\delta_{\rm ex}\simeq 10$ ergs/cm^3 could be achieved. It is important to recognize that the range of $\Delta\Omega$ that can be reached is quite small, from 0 to about 100 ergs/cm^3 in a sample cell of reasonable size.

In the second method,[37] the mixture is brought toward coexistence by moving T towards T^*. It is not a trivial matter to estimate $\Delta\Omega/(T-T^*)$; in the experiment described in Ref. 37 that ratio is perhaps[41,42] 10^6 ergs/cm^3 K. If the temperature resolution is about 1 mK, a rough estimate for the resolution in $\Delta\Omega$ is $\delta_{\rm ex}\simeq 10^3$ ergs/cm^3.

Using the present estimates for $\delta_{\rm fs}$ and $\delta_{\rm ex}$, it appears that the prewetting transition on $r_0=1000$ Å spheres would not be noticeably rounded by finite-size effects if $T-T^*$ were used to control $\Delta\Omega$. If gravity were used, finite-size rounding would completely smear the transition. However, finite-size effects would not be the only, or even the most important, cause of rounding in either case. More significant would be polydispersity in the distribution of sphere radii: a 5% width in the distribution would alone lead to a 10^4-(erg/cm^3) spread in the effective bulk field (again, using the present estimates for σ and r_0). Only for the case of monodisperse and very small spherical substrates could finite-size rounding affect experimental measurements.

VI. SUMMARY AND REMARKS

A simple interface model suggests, and study of an approximate Landau theory confirms, that the effects of substrate curvature on surface phase behavior are essentially equivalent to those due to a bulk field. In particular, for substrate radii $r_0 < \infty$ all wetting transitions are suppressed. When fluctuations are considered, one sees that for $d \leq \tau + 2$, that is, when the substrate is infinite in at most one direction, finite-size effects smear the prewetting transition. In this case, the rich surface phase diagram that one finds in planar geometry (see Fig. 1, for example) is left effectively featureless. All that remains is a bulk-driven first-order transition at bulk coexistence, where the boundary condition at infinity on the order-parameter profile undergoes a discontinuity. These conclusions are almost certainly true in any model of surface phase transitions for Ising-like systems with rough interfaces.

Only single, isolated substrates have been considered here. In practice, such as in the experiment of Beysens and Estève[5] on silica microspheres in a binary-fluid mixture, there may be many spherical substrates present. The situation is then considerably more complicated. The substrates interact, among other ways, *via* their order-parameter profiles.[43] Furthermore, capillary condensation may take place when two substrate surfaces are sufficiently close to one another, even though an isolated substrate would be on the "dry" side of the prewetting line.[44–46] The aggregation phenomenon seen in Ref. 5 was interpreted as a consequence of a prewetting transition; however, it seems equally plausible that it is related instead to capillary condensation. The aggregation line would then be a displaced image of the bulk coexistence curve, rather than a prewetting line. Further—though not especially convincing—evidence favoring this reinterpretation is that in other binary-fluid–substrate systems it is suspected that the prewetting lines are rather short and lie very close to bulk coexistence, since they have managed to completely escape detection in experiments using planar substrates.[37,47]

ACKNOWLEDGMENTS

We thank Michael E. Fisher and Stanislas Leibler for many helpful discussions; in particular, Stanislas Leibler pointed out the consequences of finite-size effects in $d=3$. Michael E. Fisher also critically reviewed the manuscript and provided invaluable advice during its preparation. Ben Widom kindly brought Ref. 25 to our attention. One of us (M.P.G.) acknowledges support from the National Science Foundation and Cornell University, and ancillary support from the National Science Foundation through the Condensed Matter Theory Program (under Grant No. DMR 81-17011).

*1987–88 address: Institute for Physical Science and Technology, College Park, MD 20742.

†Present address: Institut für Festkörperforschung, Kernforschungsanlage Jülich, Postfach 1913, 5170 Jülich, West Germany.

[1]Two recent, comprehensive reviews are K. Binder, in *Phase Transitions and Critical Phenomena,* edited by C. Domb and J. L. Lebowitz (Academic, London, 1983), Vol. 8; and D. E. Sullivan and M. M. Telo da Gama, in *Fluid Interfacial Phenomena,* edited by C. A. Croxton (Wiley, New York, 1986), p. 45.

[2]J. W. Cahn, J. Chem. Phys. **66**, 3667 (1977).

[3]C. E. Bartosch and S. Gregory, Phys. Rev. Lett. **54**, 2513 (1985).

[4]P. Taborek and L. Senator, Phys. Rev. Lett. **57**, 218 (1986).

[5]D. Beysens and D. Estève, Phys. Rev. Lett. **54**, 2123 (1985).

[6]B. V. Derjaguin, Yu. M. Popovskii, and B. A. Altoiz, J. Colloid Interface Sci. **96**, 492 (1983).

[7]R. Lipowsky, Z. Phys. B **55**, 345 (1984).

[8]P. Levinson, J. Jouffroy, and F. Brochard, J. Phys. (Paris) Lett. **46**, L21 (1985).

[9]R. Lipowsky, D. M. Kroll, and R. K. P. Zia, Phys. Rev. B **27**, 4499 (1983).

[10]E. Brézin, B. I. Halperin, and S. Leibler, J. Phys. (Paris) **44**, 775 (1983).

[11]R. Lipowsky and D. M. Kroll, Phys. Rev. Lett. **52**, 2303 (1984).

[12]D. M. Kroll and T. Meister, Phys. Rev. B **31**, 6134 (1985).

[13]M. P. Nightingale, W. F. Saam, and M. Schick, Phys. Rev. B **30**, 3830 (1984).

[14]S. Dietrich and M. Schick, Phys. Rev. B **31**, 4718 (1985).

[15]C. Ebner, W. F. Saam, and A. K. Sen, Phys. Rev. B **32**, 1558 (1985).

[16]F. P. Buff, R. A. Lovett, and F. A. Stillinger, Phys. Rev. Lett. **15**, 621 (1965).

[17]J. D. Weeks, J. Chem. Phys. **67**, 3106 (1977).

[18]R. F. Kayser, Phys. Rev. A **33**, 1948 (1986). Square and strip geometries are considered rather than spherical and cylindrical, but the corrections to σ should be nearly the same.

[19]I. E. Dzyaloshinskii, E. M. Lifshitz, and L. P. Pitaevskii, Zh. Eksp. Teor. Fiz. [Sov. Phys.—JETP **10**, 161 (1960)].

[20]I. Langmuir, Science **88**, 430 (1938).

[21]R. F. Kayser, Phys. Rev. Lett. **56**, 1831 (1986).

[22]R. Lipowsky, Phys. Rev. B **32**, 1731 (1985), contains several examples.

[23]R. Lipowsky, Phys. Rev. Lett. **52**, 1429 (1984).

[24]J. S. Rowlinson and B. Widom, *Molecular Theory of Capillarity* (Oxford University Press, New York, 1982).

[25]J. R. Henderson and J. S. Rowlinson, J. Phys. Chem. **88**, 6484 (1984), argue that there is no thermodynamically well-defined Tolman correction to the interface tension in cylindrical geometry and presumably analogous reasoning indicates that this will also be so for $\tau=1$ in any dimension.

[26]P. G. de Gennes, J. Phys. (Paris) Lett. **42**, L377 (1981).

[27]See Ref. 22. Note that Eq. (2.23) in that paper contains a misprint: $\Gamma((q-d-1)/2)$ should be replaced by $\Gamma((q-d+1)/2)$.

[28]M. P. A. Fisher and M. Wortis, Phys. Rev. B **29**, 6252 (1984).

[29]H. Nakanishi and M. E. Fisher, Phys. Rev. Lett. **49**, 1565 (1982).

[30]This is not the only conceivable strategy. For example, perturbation about $1/R_0=0$ or $\tau=0$ suggests itself, but was not attempted.

[31]Since the surface order parameter M_1 can serve to parametrize the solutions in every class, in principle one needs to consider only *one* function of a single variable.

However, the analytic form of the function depends on whether or not M_1 exceeds $H/2$, so the wet and dry classes will require separate treatment in any event.

[32]This is not a true local minimum. Using the method of Ref. 2, one sees that if M_1 is used to parametrize the solutions, then the free energy is a continuously differentiable function of M_1 even within the DPA. Thus this smallest $F_{\rm dry}$, for which $M_1=H/2$, will always exceed the free energy of nearby wet solutions with $M_1>H/2$.

[33]Note that $F_{\rm wet}$ contains powers of He^L. Therefore, it cannot serve as the interface potential, which has the generic form $V(L)=HL+V_m(L)$ where V_m is independent of H, as described after Eq. (2.1). One can obtain an interface-wall interaction V_m from the Landau theory by solving the boundary condition (3.12) for H in terms of L,H_1, and G, and integrating $H(L)\equiv -dV_m/dL$ in from $L=\infty$; see Ref. 7 and R. Lipowsky, Habilitations-Thesis, University of Munich, 1987 (unpublished).

[34]E. H. Hauge and M. Schick, Phys. Rev. B **27**, 4288 (1983).

[35]M. Abramowitz and I. A. Stegun, *Handbook of Mathematical Functions* (Dover, New York, 1972).

[36]V. Privman and M. E. Fisher, J. Appl. Phys. **57**, 3327 (1985).

[37]X. Wu, M. Schlossman, and C. Franck, Phys. Rev. B **33**, 402 (1986).

[38]O'D. Kwon, D. Beaglehole, W. W. Webb, B. Widom, J. Schmidt, J. Cahn, M. R. Moldover, and B. Stephenson, Phys. Rev. Lett. **48**, 185 (1982).

[39]In particular, W cannot change sign, for then the wetting transition would be critical rather than first order and there would be no prewetting transition to discuss.

[40]R. F. Kayser, M. R. Moldover, and J. W. Schmidt, J. Chem. Soc. Faraday Trans. 2 **82**, 1701 (1986).

[41]X. Wu and C. Franck, Phys. Rev. A (to be published).

[42]C. Franck and D. Durian (private communications). The uncertainty in this estimate is not known; the true value might differ by an order of magnitude.

[43]P. G. de Gennes, C. R. Acad. Sci. (Paris) **292**, 701 (1981).

[44]R. Evans and U. M. B. Marconi, Phys. Rev. A **32**, 3817 (1985).

[45]R. Lipowsky and G. Gompper, Phys. Rev. B **29**, 5213 (1984).

[46]H. Nakanishi and M. E. Fisher, J. Chem. Phys. **78**, 3279 (1983).

[47]J. W. Schmidt and M. R. Moldover, J. Chem. Phys. **84**, 4563 (1986).